

Original article

Estimated ultimate recovery prediction of fractured horizontal wells in tight oil reservoirs based on deep neural networks

Shangui Luo¹, Chao Ding², Hongfei Cheng³, Boning Zhang^{1,4}, Yulong Zhao¹^{*}, Lingfu Liu⁵

¹State Key Laboratory of Oil & Gas Reservoir Geology and Exploitation, Southwest Petroleum University, Chengdu 610500, P. R. China

²Fengcheng Oilfield Operation Area of PetroChina Xinjiang Oilfield Company, Karamay, Xinjiang 834000, P. R. China

³Heavy Oil Development Company of PetroChina Xinjiang Oilfield Company, Karamay, Xinjiang 834000, P. R. China

⁴Chengdu North Petroleum Exploration and Development Technology Company Limited, Chengdu 610051, P. R. China

⁵Department of Chemical Engineering, University of Wyoming, Laramie, WY 82071, USA

Keywords:

Tight oil reservoirs
fractured horizontal wells
deep neural network
hyperparameter optimization
estimated ultimate recovery

Cited as:

Luo, S., Ding, C., Cheng, H., Zhang, B., Zhao, Y., Liu, L. Estimated ultimate recovery prediction of fractured horizontal wells in tight oil reservoirs based on deep neural networks. *Advances in Geo-Energy Research*, 2022, 6(2): 111-122.

<https://doi.org/10.46690/ager.2022.02.04>

Abstract:

Accurate estimated ultimate recovery prediction of fractured horizontal wells in tight reservoirs is crucial to economic evaluation and oil field development plan formulation. Advances in artificial intelligence and big data have provided a new tool for rapid production prediction of unconventional reservoirs. In this study, the estimated ultimate recovery prediction model based on deep neural networks was established using the data of 58 horizontal wells in Mahu tight oil reservoirs. First, the estimated ultimate recovery of oil wells was calculated based on the stretched exponential production decline model and a five-region flow model. Then, the calculated estimated ultimate recovery, geological attributes, engineering parameters, and production data of each well were used to build a machine learning database. Before the model training, the number of input parameters was reduced from 14 to 9 by feature selection. The prediction accuracy of the model was improved by data normalization, the early stopping technique, and 10-fold cross validation. The optimal activation function, hidden layers, number of neurons in each layer, and learning rate of the deep neural network model were obtained through hyperparameter optimization. The average determination coefficient on the testing set was 0.73. The results indicate that compared with the traditional estimated ultimate recovery prediction methods, the established deep neural network model has the strengths of a simple procedure and low time consumption, and the deep neural network model can be easily updated to improve prediction accuracy when new well information is obtained.

1. Introduction

Horizontal well drilling and stimulation technology promote the development of unconventional oil and gas resources such as tight oil (Hughes, 2013; Aguilera, 2014; Meng et al., 2020; Li et al., 2020). However, owing to tight oil's inherent properties of low porosity, low permeability, and strong heterogeneity, along with the complexity of the hydraulic fracture network (Dontsov et al., 2020; Qin et al., 2020), production prediction in tight reservoirs is still a challenge. As shown in Table 1, the estimated ultimate recovery (EUR) prediction methods of a single well in a tight reservoir mainly include the

empirical decline curve analysis (Liang et al., 2020), modern production decline analysis (Boogar et al., 2011), analytical model method (Brown et al., 2009; Stalgorova et al., 2013), and numerical simulation method (Khamidullin et al., 2017; Ji et al., 2020; Luo et al., 2021). The empirical decline curve analysis method uses an empirical mathematical model to fit the production data. Common empirical decline curve analysis methods include Arps's model (Arps, 1945), the stretched exponential production decline (SEPD) model (Valko, 2009), Duong's model (Duong, 2010), Wang's model (Wang et al., 2017), the logistic growth model (LGM) (Clark et al., 2011), and Hsieh's model (Hsieh et al., 2001). Common modern

Table 1. EUR prediction method for fractured horizontal wells.

EUR prediction method	Function	Applicable flow pattern	Data needed		
Empirical production decline model	Arps's model	Production/EUR prediction	Boundary-dominated flow		
	SEPD model	Production/EUR prediction	Linear flow/boundary-dominated flow		
	Duong's model	Production/EUR prediction	Linear flow	Production data	
	Wang's model	Production/EUR prediction	Linear flow		
	LGM	Production/EUR prediction	Linear flow		
	Hsieh's model	Production/EUR prediction	Linear flow		
Modern production decline analysis	Blasingame	EUR prediction	Transient flow/boundary-dominated flow		Fluid properties, geological parameters, production data.
	Fetkovich	EUR prediction	Boundary-dominated flow		
	FMB	EUR prediction	Boundary-dominated flow		
Analytical model	A three-region model	Production/pressure/EUR prediction	All flow patterns	Fluid properties, geological parameters, construction parameters, production data.	
	A five-region model	Production/pressure/EUR prediction	All flow patterns		
Numerical simulation	/	Production/pressure/EUR prediction	All flow patterns		

production decline analysis methods include the Blasingame type curve method, Fetkovich type curve method, and flowing material balance (FMB) method (Fetkovich, 1980; Mattar et al., 1998; Cui et al., 2021). Combined with the unsteady seepage theory and empirical decline method, according to oil well production data, the relationship between pressure and production is analyzed using modern production decline typical curve fitting. Then, reservoir parameters and well control reserves are obtained by typical curve fitting, and the EUR is calculated. Both analytical model method and numerical simulation are based on reservoir seepage theory, which can describe the complex seepage process. However, these approaches require many physical parameters, and it is difficult to establish and solve them.

Over the past few years, with the application and expansion of artificial intelligence in the petroleum industry (Broni-Bediako et al., 2019; Kuang et al., 2021; Yavari et al., 2021; Wood, 2022), it has become possible to set up a fast and accurate oil well production forecasting method based on machine learning. Mohaghegh (2011) considered that reservoir simulation and the production prediction method based on machine learning can be split into the top-down model and surrogate reservoir model according to the data sources during model development. Bansal et al. (2013) used an artificial neural network (ANN) to describe the complicated relationship between the logging curve, seismic data, completion parameters, and production dynamic characteristics. Then, they predicted the cumulative oil and gas production of wells in tight reservoirs within 2 years. Cao et al. (2016) used ANN to forecast the future production performance of Eagle Ford shale wells. They believed that the data-driven

production prediction method is more comprehensive than the decline curve analysis and takes much less time than the numerical simulation method. Lee et al. (2019) used long short-term memory to forecast the production change of shale gas wells in the coming month. They found that the prediction accuracy of the two-feature case considering production data and SI cycle was higher than that of the single-feature case considering production data only. Wang et al. (2019) used a deep neural network (DNN) to forecast the cumulative oil production of shale oil horizontal wells at 6 and 18 months, and believed that the amount of proppant would have the greatest influence on production. Chen et al. (2020) predicted the test output of shale gas horizontal wells on the basis of the genetic algorithm-back propagation neural network, and its prediction accuracy was significantly higher than that of the multiple linear regression model. Liu et al. (2021) designed a shale gas well EUR prediction algorithm on the basis of deep learning in light of geological data, fracturing stimulation data, production data, and EUR calculation results. They found that the change and number of input parameters, network structure, and hyperparameters had an impact on the prediction accuracy of EUR. Niu et al. (2022) predicted the shale gas well EUR based on a variety of machine learning algorithms using early data. The research results show that the early production data had the greatest impact on the EUR. In addition, because the support vector machine is applicable for small data sets, it is the most trustworthy model.

In sum, recent research on yield prediction in machine learning has mainly focused on early yield and production dynamics prediction. However, EUR prediction for unconventional reservoirs based on machine learning has only

emerged in recent years. Therefore, combined with the reservoir engineering method and deep learning, we established an EUR prediction model of fractured horizontal wells in tight oil reservoirs on the basis of the DNN. In the process of model development, feature selection, data normalization, early stopping technology, and 10-fold cross validation method were adopted to improve the computational efficiency and prediction accuracy of the DNN model. On this basis, the impact of hyperparameters on the performance of DNN model was examined.

2. Database establishment

2.1 EUR calculation based on empirical decline model

The empirical decline method and analytical model method were first used to calculate the EUR to provide the initial EUR for database establishment. The well spacing of fractured horizontal wells in well block Ma18 of the Mahu oil field is mainly 300 to 350 m. Microseismic monitoring shows that the hydraulic fracture length is between 61 and 236 m. In addition, the phenomenon of frac hits in adjacent horizontal wells occasionally occurs during the fracturing operation. Meanwhile, the production dynamic of wells shows that the stable production stage in the well area is short, and the decline rate of production is fast. All these indicate that the oil wells in well block Ma18 will quickly reach a boundary flow state. The oil wells used in this study have a production time of about 1 year, which meets the conditions of the empirical decline model to predict the EUR. Empirical decline curve analysis is a common method of production prediction in an oil field. However, owing to the variety of decline models and the diversity of Mahu tight conglomerate reservoirs, the optimization of decline models is essential. We divided the actual production data of the oil well into a fitting data section and production prediction verification section. The root mean square error (RMSE) of the actual value and predicted value was used as the evaluation index:

$$\text{RMSE} = \sqrt{\frac{1}{n} \sum_{i=1}^n (\hat{q}_i - q_i)^2} \quad (1)$$

where q_i is the actual production data, \hat{q}_i is the predicted production data, and n is the number of data points that were effectively decremented.

Based on the literature review mentioned above, this study mainly evaluated five empirical decline models (Fig. 1). Taking horizontal well M01 in well block Ma18 of the Mahu oil field as an example, when the effective fitting time of production data was 100 days, the production prediction of various decline models was not ideal. In other words, when the fitting stage was short, all models would have obvious deviations in the prediction stage. This may mean that the well had not yet reached the boundary flow stage. As the effective fitting time increased, however, the predicted RMSE of each decline model decreased (Fig. 2). When the fitting stage reached 200 days, the SEPD model showed the best prediction effect and high stability. Therefore, the SEPD model was used to calculate the

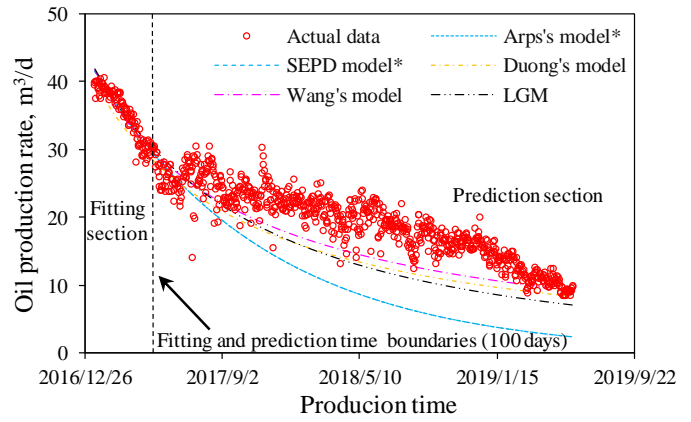


Fig. 1. Schematic of production fitting and prediction validation for different decline models of well M01 (*the prediction curves of the two models almost coincide).

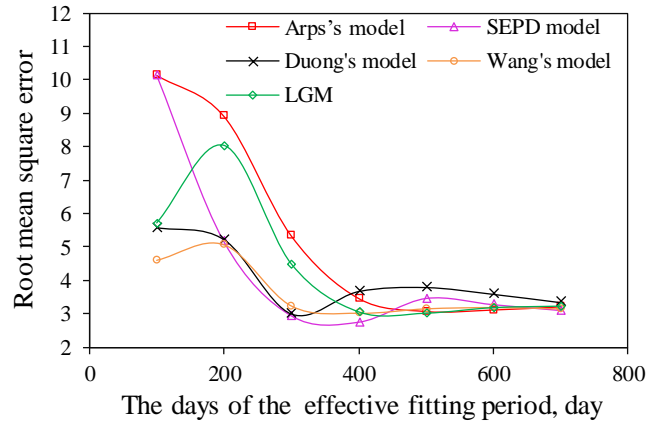


Fig. 2. Relationship curves between the RMSE of prediction data of different decline models and the effective fitting time of well M01.

EUR among various decline models. In the calculation of the EUR based on the fitted decline model, when the daily oil production was reduced to 0.5 m³/d, the cumulative oil production volume was considered as the EUR of each well.

2.2 EUR calculation based on analytical model

When the production data met the prediction conditions of empirical decline model, the SEPD model was used to predict EUR. However, when there was no obvious decline stage of fractured horizontal wells or the decline law was damaged, the five-region linear flow model of fractured horizontal wells was used to calculate the EUR. This model was first proposed by Stalgorova and Mattar (2013). In their research, a detailed formula derivation and solving process were given, so this study only gives a brief introduction to the five-region model. As shown in Fig. 3, because of the symmetry of the system, only one quarter of the space between the fractures needs to be computed. Flow in this model is regarded as a combination of five linear flows within contiguous regions. Regions 2, 3, and 4 represent the original reservoir rocks, which have identical properties. Region 1 represents the branching fracture region

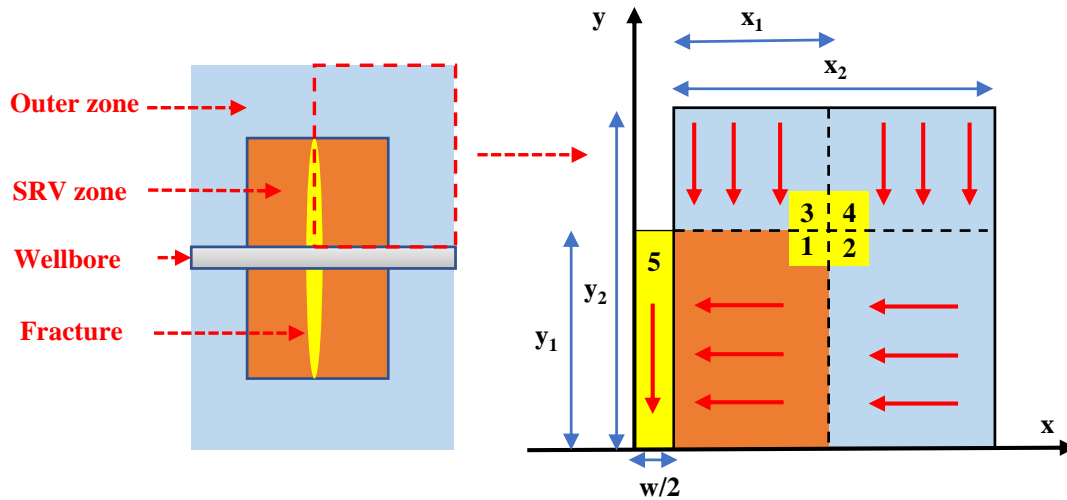


Fig. 3. Schematic diagram of the five-region physical model of fractured horizontal well in tight reservoir.

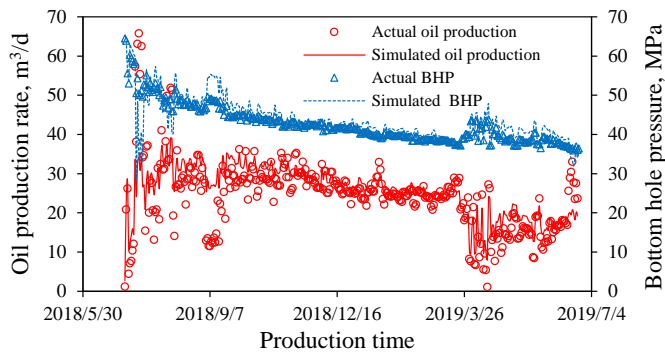


Fig. 4. Production history fitting curve of analytical model of well M02.

adjacent to the hydraulic fracture. Therefore, region 1 is a higher-permeability zone, which is the stimulated reservoir volume (SRV) zone. Region 5 represents the hydraulic fracture region. One-dimensional flow solutions for each region are formulated and then coupled by applying flux and pressure continuity across the boundaries between regions. As shown in Fig. 3, the horizontal well is along the x -direction, the hydraulic fracture is along the y -direction, x_1 is half of the width of the SRV zone, x_2 is half the distance between fractures, y_1 is half of the hydraulic fracture length, and y_2 is half of the well spacing.

In the practical application, parameters such as the model boundary, horizontal well length, initial pressure, initial water saturation, porosity, fluid properties, and number of hydraulic fractures were first input according to the actual data of horizontal well. Then, the production history fitting was realized by adjusting the hydraulic fracture length, fracture conductivity, permeability of SRV area, net pay, and other parameters (Fig. 4). Based on the fitted analytical model, the production system of the first fixed daily oil production and then the fixed bottom hole pressure was used to continue the prediction. As with the empirical decline model, when the daily oil production was reduced to 0.5 m³/d, the cumulative

oil production volume was considered as the EUR of the fractured horizontal well.

2.3 Machine learning database

The data of this study come from the fractured horizontal wells in well block Ma18 of the Mahu oil field. The production of oil wells in tight reservoirs is affected by geological properties, engineering parameters, and the production system. Therefore, the porosity, matrix permeability (measured with gas), oil saturation, brittleness index, Young's modulus, Poisson's ratio, length of horizontal section, thickness of the class I reservoir, number of fracturing stages, cluster spacing, fracturing fluid volume per stage, sand volume per stage, soaking time, production rate in the first year, and the EUR of 58 horizontal wells were counted. The statistical characteristics of each parameter are shown in Table 2. As shown in Fig. 5, except for the soaking time and Poisson's ratio, other parameters showed a certain normal distribution characteristic. Normal distribution is the theoretical basis of many statistical analysis methods. For example, correlation analysis and regression analysis require that the analysis index obey normal distribution or approximate normal distribution. Therefore, the parameters selected in this study had a high analytical value. These data were used to establish the DNN model.

3. Establishment of the DNN model

3.1 DNN

The DNN is an important branch in the field of artificial intelligence. Hinton et al. (2006) adopted the scheme of unsupervised pre-training to initialize the weights and supervised training to fine-tune the whole network, which solved the problem of gradient disappearance in deep network training. Then, the DNN entered a period of rapid development. As shown in Fig. 6, both the DNN and traditional neural network system are composed of the input layer, the hidden layer, and the output layer. The DNN contains multiple hidden layers,

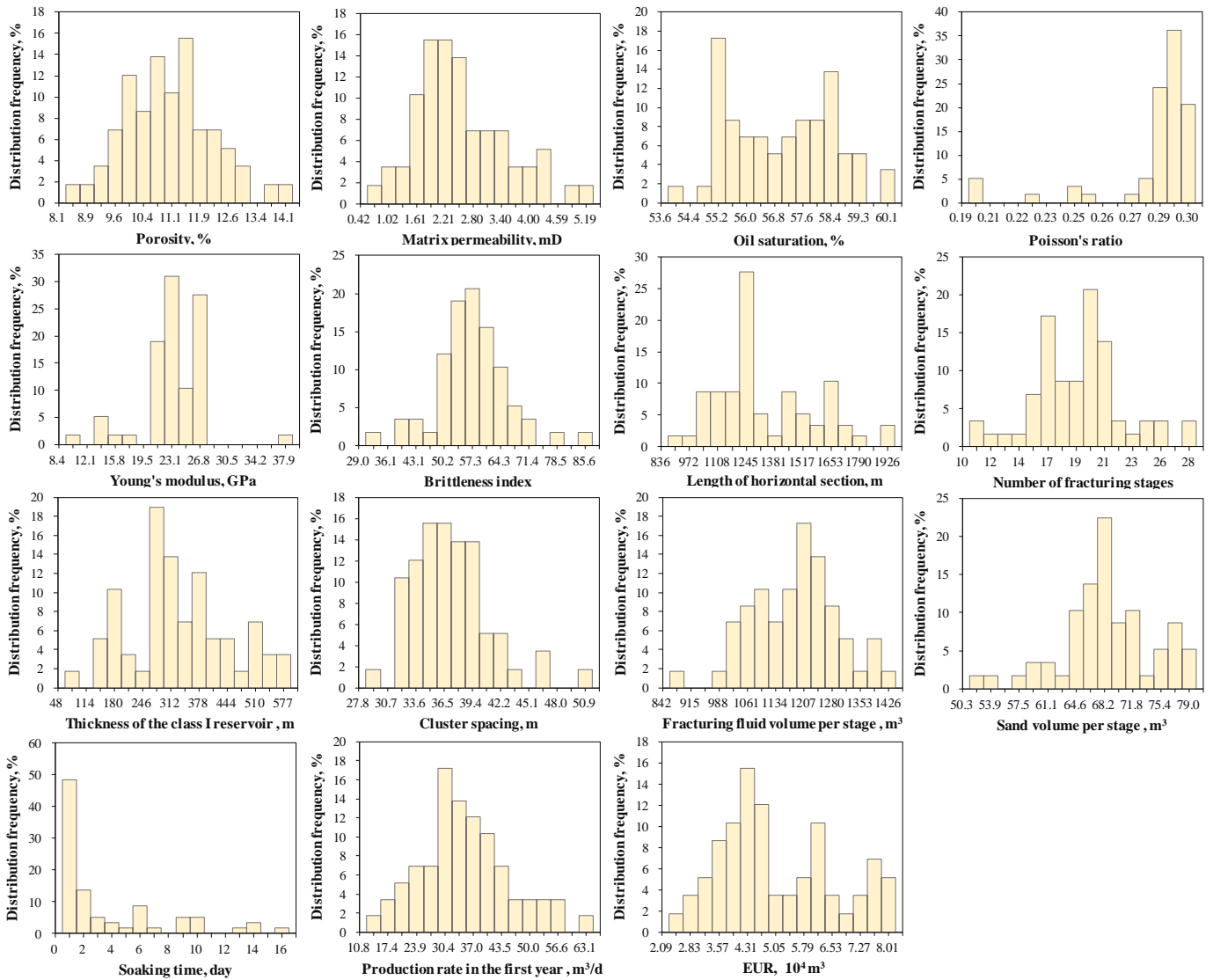


Fig. 5. Distribution frequency of each parameter in the database.

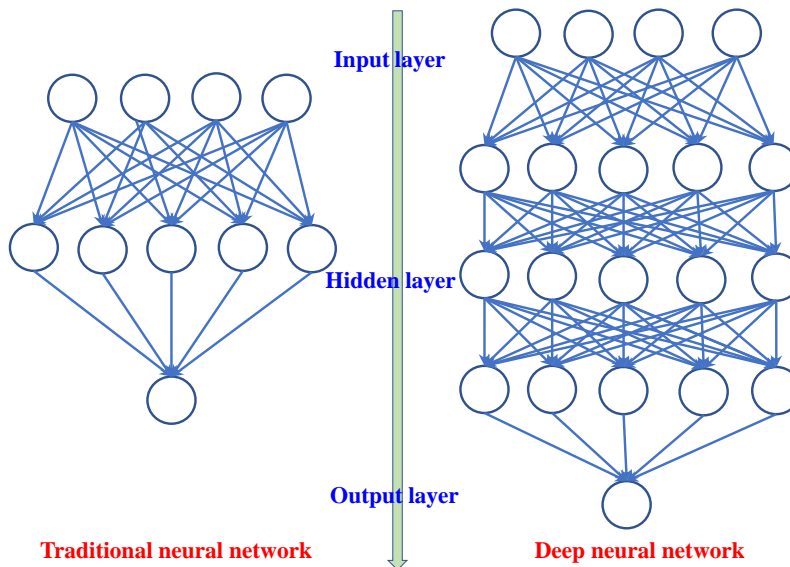


Fig. 6. Structure comparison between traditional neural network and DNN.

Table 2. Statistical characteristics of each parameter of fractured horizontal wells in well block Ma18.

Parameter type	Parameter	Range	Mean	Standard deviation
Geological property	Porosity (%)	8.49-14.13	10.85	1.16
	Matrix permeability (measured with gas) (mD)	0.72-5.19	2.4	0.97
	Oil saturation (%)	53.96-60.07	56.85	1.52
	Poisson's ratio	0.2-0.3	0.28	0.024
	Young's modulus (Gpa)	10.23-37.9	22.39	4.19
	Brittleness index	32.53-85.55	55.28	8.84
Engineering parameter	Length of horizontal section (m)	904-1926	1302	243.63
	Number of fracturing stages	11-28	19	3.66
	Thickness of the class I reservoir (m)	80.63-576.5	316.53	117.89
	Cluster spacing (m)	29.27-50.9	36.56	4.08
	Fracturing fluid volume per stage (m ³)	878.3-1426.3	1169.3	110.98
	Sand volume per stage (m ³)	52.11-78.25	67.67	5.81
Production	Soaking time (day)	1-16	3.74	4.02
	Production rate in the first year (m ³ /d)	14.1-63.09	33.56	10.42
	EUR (10 ⁴ m ³)	2.46-8.01	4.9	1.52

and the learning ability of the model is greatly improved. In addition, more complicated network structures and better learning algorithms promote the development of deep learning (Bouwman et al., 2019). In this study, we developed DNN models based on MATLAB to forecast the EUR of oil wells in tight oil reservoirs. At the same time, feature selection, data normalization, early stopping, cross-validation, and the Adam optimizer were used to improve the forecasting accuracy and convergence speed.

3.2 Feature selection

Feature selection in machine learning can promote data visualization and understanding as well as reduce redundant input dimensions to enhance the prediction performance of the ANN model (Guyon et al., 2003). Based on the established database, the main control factors analysis of the EUR and feature selection were conducted. To compare the correlation of each feature parameter, the Pearson correlation coefficient, shown in Eq. (2), was used to realize feature selection. According to the calculation results (Fig. 7), the DNN model includes nine characteristic input parameters (matrix permeability, production rate in the first year, porosity, oil saturation, thickness of class I reservoir, cluster spacing, sand volume per stage, fluid volume per stage, and soaking time) with the strongest correlation with the EUR. At the same time, it was found that among the nine parameters, EUR was negatively correlated with cluster spacing and Poisson's ratio, and positively correlated with other parameters. In addition, the factors with higher correlation coefficients were mostly geological parameters, which indicates that geological factors have a greater impact on the EUR than engineering factors.

$$r = \frac{\sum_{i=1}^n (X_i - \bar{X})(Y_i - \bar{Y})}{\sqrt{\sum_{i=1}^n (X_i - \bar{X})^2} \sqrt{\sum_{i=1}^n (Y_i - \bar{Y})^2}} \quad (2)$$

where r is the Pearson correlation coefficient between input parameters and output parameters; X_i is the i^{th} value of parameter X ; \bar{X} is the average value of parameter X ; Y_i is the i^{th} value of parameter Y ; \bar{Y} is the average value of parameter Y .

3.3 Data normalization

As shown in Table 1, the dimensions and value ranges of input parameters were considerably different, leading to the decrease of convergence speed or even failure of convergence when using the gradient descent method. For the purpose of improving the training efficiency of the neural network model, the Min-Max normalization method was used to standardize all input and output parameters so that the value range of each parameter was mapped to [0,1]:

$$x_n = \frac{x - x_{\min}}{x_{\max} - x_{\min}} \quad (3)$$

where x_n is the normalization parameter; x is the actual parameter; x_{\min} is the minimum value of variable x ; x_{\max} is the maximum value of variable x .

3.4 Regularization technique

When there is little training sample data or the model is too complex, the overfitting problem of the model can occur. Therefore, regularization technology is often used in machine learning to avoid overfitting. The regularization method is a

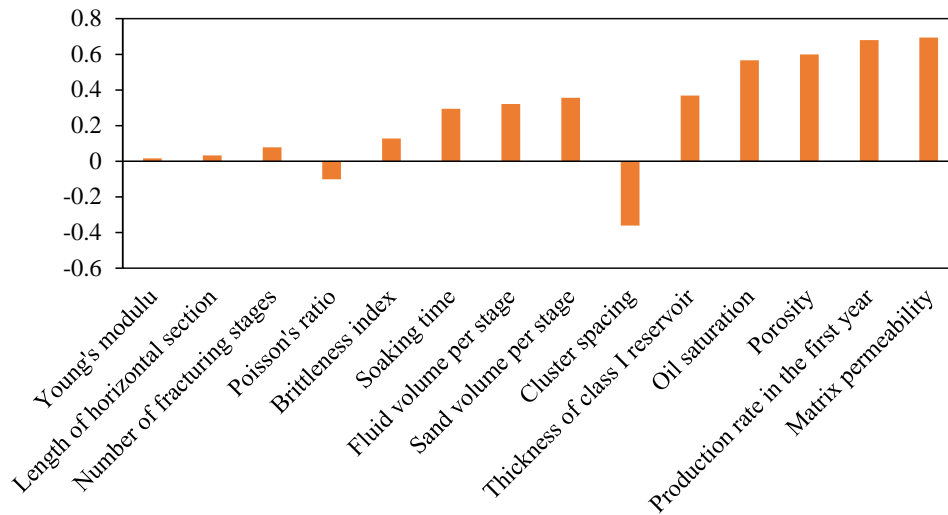


Fig. 7. Ranking chart of Pearson correlation coefficient between each parameter and EUR.

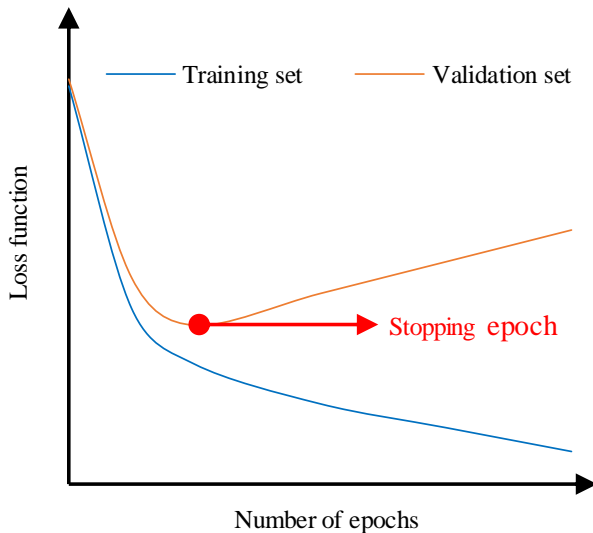


Fig. 8. Illustration of early stopping technique.

general term for a class of methods to avert overfitting and enhance the generalization performance of the DNN model by introducing additional information into the original loss function. Regularization techniques commonly used in deep learning include early stopping, data augmentation, L1 and L2 regularization, and dropout (Srivastava et al., 2014). This study used early stopping to solve the overfitting problem. As shown in Fig. 8, the validation error is reduced at the initial stage of the training process. When the model is overfitted, the training error decreases continuously, but the validation error starts to increase. Once the validation error begins to increase after several iterations, the training procedure stops. Then, the model returns to the weight and deviation with the smallest validation error.

3.5 K-fold cross validation

K-fold cross validation is an effective method to evaluate the generalization performance of the model in machine learning (Arlot et al., 2010). When there is little sample data,

cross validation can make the best of the whole sample data set to train the model. Cross-validation is used to randomly separate the whole data set into k mutually exclusive subsets of the equal size, and each subset should hold the uniformity of data distribution as far as possible. After that, the $k-1$ subset is selected as the training set, and the residual 1 subset is treated as the testing set to evaluate the performance of the model. After traversing K subsets, K training and testing are conducted. The final return is the average of these K test results. Although this method increases the amount of calculation, it makes full use of the whole data set, and the model is more reliable. Obviously, the stability and fidelity of the evaluation results of cross-validation method largely depend on the value of K (Zhou, 2016). Generally, the value of K is 5, 10, and 20. As shown in Fig. 9, we selected the most commonly used 10-fold cross validation method to avoid the overfitting problem in the learning process of small sample data.

3.6 Adam optimizer

Machine learning is a process of constantly updating a set of parameters. The objective function is optimized by updating the parameters using the optimization algorithm. Gradient descent algorithm is a commonly used algorithm. It optimizes the objective function by following the steepest descent direction. At present, mainstream optimizers based on gradient descent include stochastic gradient descent with momentum and Adam. Other algorithms are mostly aimed at the improvement of these two kinds of algorithms. Among them, Adam is a first-order adaptive momentum stochastic optimization algorithm, which can iteratively update the neural network weight based on the training data (Khan et al., 2021). The Adam algorithm is the combination of the Momentum and RMSProp algorithms. It has the advantages of easy implementation, high computing efficiency, and low memory demand. We used the Adam algorithm to update the weight and deviation of the DNN model, and its update rules are described as follows:

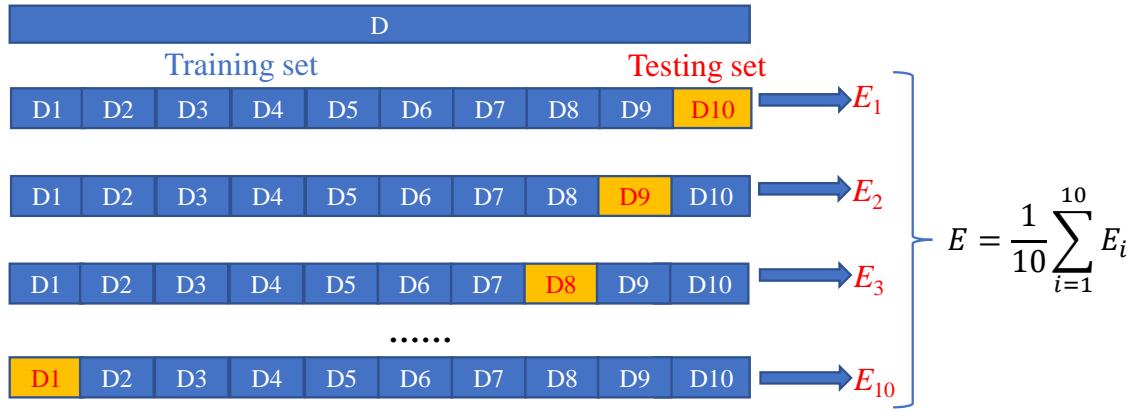


Fig. 9. Schematic diagram of 10-fold cross validation.

Table 3. Value table of hyperparameter optimization.

Optimization parameters	Value
Type of activation function	purelin, logsig, tansig
Number of hidden layers	1, 2, 3, 4, 5
Number of neurons	5, 10, 15, 20, 30, 40, 50, 100, 200, 300, 400
Learning rate	0.00001, 0.00005, 0.0001, 0.0002, 0.0005, 0.001, 0.002, 0.003, 0.004, 0.005, 0.01, 0.02, 0.05, 0.1, 0.5

$$\theta_t = \theta_{t-1} - \frac{\eta}{\sqrt{\hat{v}_t} + \epsilon} \hat{m}_t \quad (4)$$

$$\hat{m}_t = \frac{m_t}{1 - \beta_1^t} \quad (5)$$

$$\hat{v}_t = \frac{v_t}{1 - \beta_2^t} \quad (6)$$

$$m_t = \beta_1 m_{t-1} + (1 - \beta_1) g_{t-1} \quad (7)$$

$$v_t = \beta_2 v_{t-1} + (1 - \beta_2) g_{t-1}^2 \quad (8)$$

where t is number of steps updated; η is learning rate; θ represents the parameters to be updated; g is gradient of loss function to θ ; m_t is the first-order matrix of gradient; v_t is the second-order matrix of gradient g ; \hat{m}_t is the offset correction of m_t ; \hat{v}_t is the offset correction of v_t ; β_1 , β_2 , and ϵ are the hyperparameter of the algorithm. Generally, β_1 is 0.9, β_2 is 0.999, and ϵ is $10e^{-8}$.

4. Results and discussion

4.1 Hyperparameter optimization of the DNN model

Two kinds of parameters are often involved in machine learning. One is the parameters of the algorithm, also known as hyperparameters, which are usually less than 10. The other is the parameters of the model, which are usually large. Hyperparameters are usually generated by manually setting multiple parameter candidate values. The parameters of the model automatically generate multiple candidate models through learning, which is completed by the Adam optimizer mentioned earlier.

Owing to the 10-fold cross validation, the average mean square error of 10 neural network models established in the training process was taken as the loss function. The data set after feature selection was used to optimize the network structure and hyperparameters of the DNN model. Table 3 lists the parameter values. Given the hyperparameters, it took less than 1 second for a computer with 12 CPUs to train a model.

The box plot contains statistical information such as the average value and distribution range of the objective function, which is convenient to compare the performance and stability of the model. Optimization results show that for the DNN model, the performance of purelin activation function was very poor, and the performance of logsig activation function was slightly better than tansig activation function (Fig. 10). As shown in Fig. 11, with the increase in the number of hidden layers, the objective function first diminished rapidly. When the number of layers was greater than 3, the objective function fluctuated slightly. Then, based on the three hidden layers, the number of neurons in each layer was further optimized. The objective function was first diminished with the increase in the number of neurons (Fig. 12). When the number of neurons was greater than 20, the objective function fluctuated slightly. When the number of neurons was 50, the prediction accuracy was the highest. The learning rate is also an important hyperparameter of the DNN model. The objective function first diminished slowly with the increase in the learning rate. However, when the learning rate was greater than 0.0005, the objective function was augmented rapidly (Fig. 13). The results show that 0.0005 was the best learning rate. Based on above analysis, the optimal hyperparameters of the DNN model are shown in Table 4.

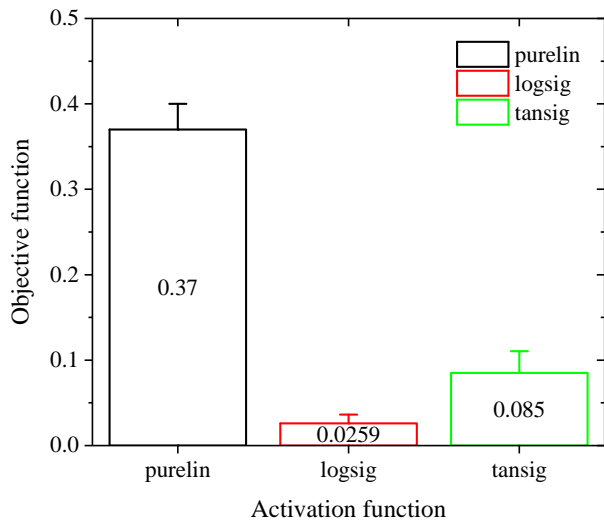


Fig. 10. Influence of activation function on neural network performance.

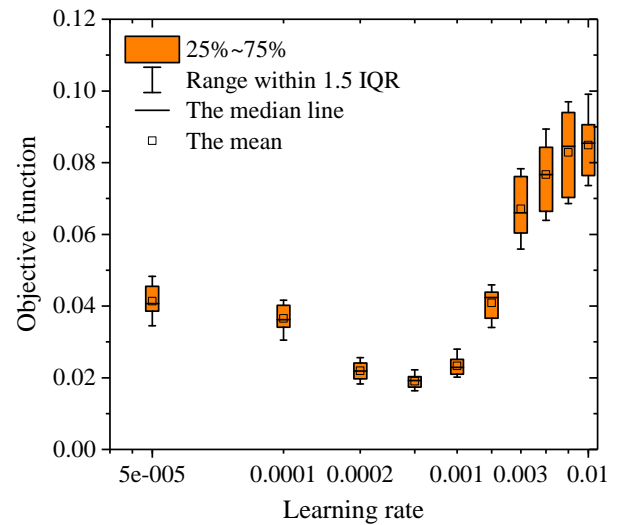


Fig. 13. Influence of learning rate on neural network performance.

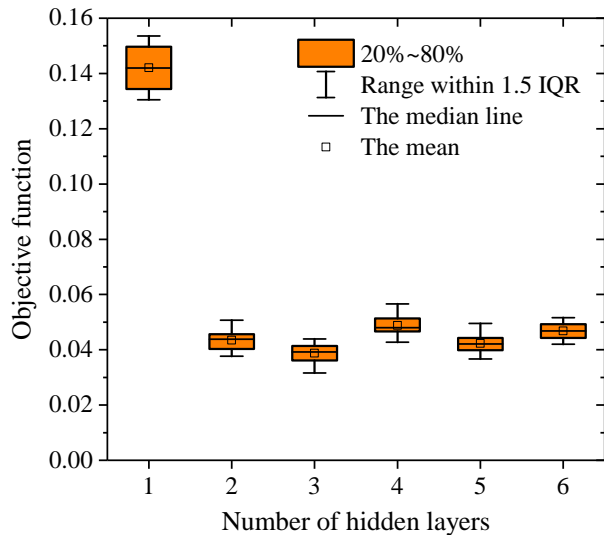


Fig. 11. Influence of hidden layers on neural network performance.

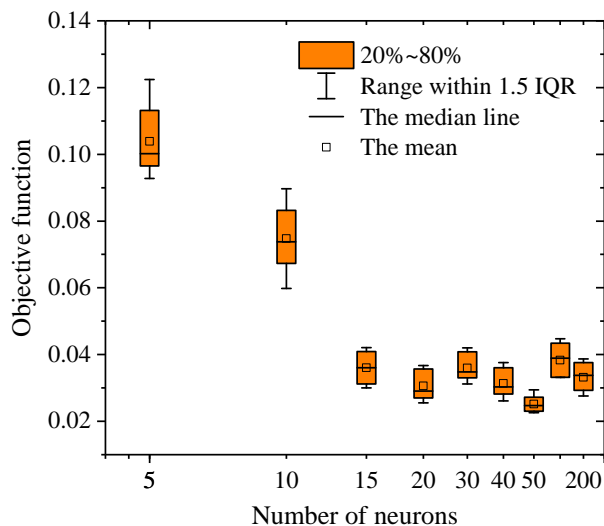


Fig. 12. Influence of number of neurons on neural network performance.

Table 4. Hyperparameter optimization results of DNN model.

Hyperparameter	The optimal value
Type of activation function	Logsig
Number of hidden layers	3
Number of neurons per layer	50
Learning rate	0.0005

4.2 EUR prediction based on the model

First, 10% of the total data set was stochastically selected as the testing set. The remaining 90% data were randomly divided into 10 copies, and the EUR prediction model was established by 10-fold cross validation technology. The optimal DNN models were established by using the hyperparameters shown in Table 4. The result for one of these models is shown in Fig. 14. The average determination coefficient of the 10 DNN models on the testing set was 0.73, showing that the EUR prediction model based on DNN had strong prediction performance. As shown in Table 5, the average mean square error of the testing set on the DNN model was 0.51, while the average mean square error on the multiple linear regression model was 1.09. The prediction accuracy of EUR based on DNN model was significantly higher than that of the simple multiple linear regression model.

5. Conclusions

This study established a EUR prediction model of fractured horizontal wells in tight oil reservoirs on the basis of the DNN. Through research, the following conclusions were drawn:

- 1) The combination of traditional EUR prediction methods and machine learning method to establish the DNN model is an effective means to achieve rapid EUR forecasting of fractured horizontal wells. In the Mahu tight reservoir,

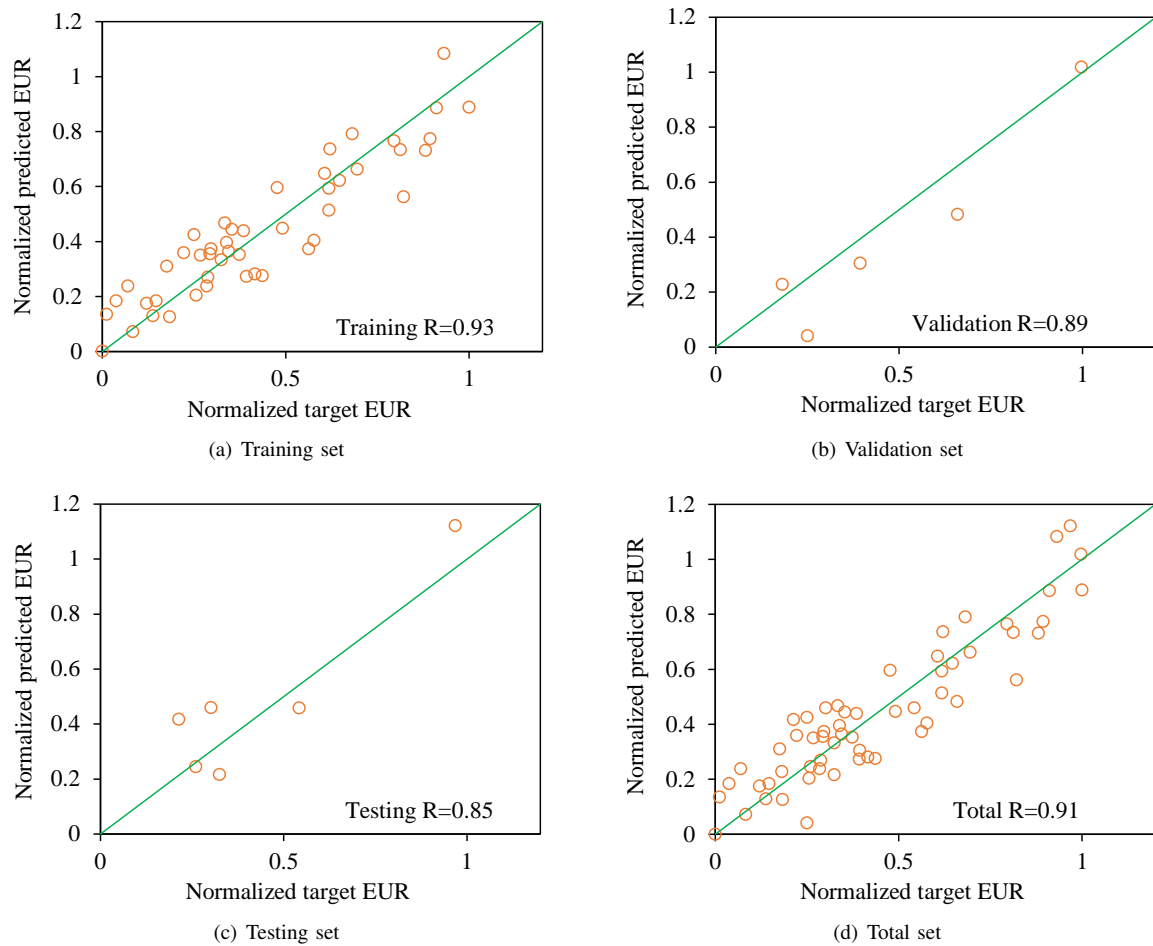


Fig. 14. Comparison between the normalized EUR predicted value and actual EUR.

Table 5. Comparison of prediction results in DNN and multiple linear regression model.

Number	Actual EUR (10^4 m^3)	DNN prediction (10^4 m^3)	Mean square error	Linear regression model prediction (10^4 m^3)	Mean square error
1	3.92	3.32	0.36	4.27	0.12
2	7.86	7.11	0.56	6.64	1.49
3	4.16	4.48	0.1	5.15	0.98
4	5.48	4.94	0.29	4.41	1.14
5	3.66	4.87	1.46	5.24	2.5
6	4.28	3.73	0.3	4.82	0.29
Average value	4.89	4.74	0.51	5.09	1.09

the SEPD model and five-region linear flow model are reliable methods for EUR prediction among the traditional methods.

- Feature selection shows that the EUR of horizontal wells in tight oil reservoirs is mainly affected by nine characteristic parameters. These include matrix permeability, daily oil production in the first year, porosity, oil saturation, thickness of the class I reservoir, cluster spacing, fracturing fluid volume per stage, sand volume per stage,
- and soaking time. At the same time, the EUR is negatively correlated with cluster spacing and Poisson's ratio, and positively correlated with other parameters.
- For small sample data learning, using early stopping and 10-fold cross validation technology can effectively avoid the overfitting problem of EUR prediction model. The continuous tracking and import of oil field data and the expansion of the sample size of the database can significantly increase the prediction accuracy of the DNN

model.

- 4) The activation function, the number of hidden layers and neurons per layer, and the learning rate all affect the performance of the DNN model. The best DNN model obtained by hyperparameter optimization requires a logsig activation function, 3 hidden layers, 50 neurons per layer, and a learning rate of 0.0005. Compared with multiple linear regression model, the prediction accuracy of the DNN model is twice that of the linear regression model.

Acknowledgement

This work was supported by National Natural Science Foundation of China (Key Program) (No. 51534006) and National Natural Science Foundation of China (Nos. 51874251 and 52074235).

Conflict of interest

The authors declare no competing interest.

Open Access This article is distributed under the terms and conditions of the Creative Commons Attribution (CC BY-NC-ND) license, which permits unrestricted use, distribution, and reproduction in any medium, provided the original work is properly cited.

References

- Aguilera, R. Flow units: From conventional to tight-gas to shale-gas to tight-oil to shale-oil reservoirs. *SPE Reservoir Evaluation & Engineering*, 2014, 17(2): 190-208.
- Arlot, S., Alain, C. A survey of cross-validation procedures for model selection. *Statistics Surveys*, 2010, 4: 40-79.
- Arps, J. J. Analysis of decline curves. *Transactions of the AIME*, 1945, 160(1): 228-247.
- Bansal, Y., Ertekin, T., Karpyn, Z., et al. Forecasting well performance in a discontinuous tight oil reservoir using artificial neural networks. Paper SPE 164542 Presented at SPE Unconventional Resources Conference, Woodlands, Texas, USA, 10-12 April, 2013.
- Boogar, A. S., Gerami, S., Masihi, M. Investigation into the capability of a modern decline curve analysis for gas condensate reservoirs. *Scientia Iranica*, 2011, 18(3): 491-501.
- Bouwmans, T., Javed, S., Sultana, M., et al. Deep neural network concepts for background subtraction: A systematic review and comparative evaluation. *Neural Networks*, 2019, 117: 8-66.
- Broni-Bediako, E., Fuseini, N. I., Akoto, R. N. A., et al. Application of intelligent well completion in optimising oil production from oil rim reservoirs. *Advances in Geo-Energy Research*, 2019, 3(4): 343-354.
- Brown, M. L., Ozkan, E., Raghavan, R. S., et al. Practical solutions for pressure-transient responses of fractured horizontal wells in unconventional shale reservoirs. *SPE Reservoir Evaluation & Engineering*, 2009, 14(6): 663-676.
- Cao, Q., Banerjee, R., Gupta, S., et al. Data driven production forecasting using machine learning. Paper SPE 180984 Presented at SPE Argentina Exploration & Production of Unconventional Resources Symposium, Buenos Aires, Argentina, 1-3 June, 2016.
- Chen, J., Huang, H., Liu, J., et al. Production predicting technology of shale gas fracturing horizontal well in Changning area based on the GA-BP neural network model. *Science Technology and Engineering*, 2020, 20(5): 1851-1858. (in Chinese)
- Clark, A. J., Lake, L. W., Patzek, T. W. Production forecasting with logistic growth models. Paper SPE 144790 Presented at SPE Annual Technical Conference and Exhibition, Denver, Colorado, USA, 30 October-2 November, 2011.
- Cui, Y., Jiang, R., Gao, Y. Blasingame decline analysis for multi-fractured horizontal well in tight gas reservoir with irregularly distributed and stress-sensitive fractures. *Journal of Natural Gas Science and Engineering*, 2021, 88: 103830.
- Dontsov, E. V., Suarez-Rivera, R. Propagation of multiple hydraulic fractures in different regimes. *International Journal of Rock Mechanics and Mining Sciences*, 2020, 128: 104270.
- Duong, A. N. An unconventional rate decline approach for tight and fracture-dominated gas wells. Paper SPE 137748 Presented at Canadian Unconventional Resources and International Petroleum Conference, Calgary, Alberta, Canada, 19-21 October, 2010.
- Fetkovich, M. J. Decline curve analysis using type curves. *Journal of Petroleum Technology*, 1980, 32(6): 1065-1077.
- Guyon, I., Elisseeff, A. An introduction to variable and feature selection. *Journal of Machine Learning Research*, 2003, 3(3): 1157-1182.
- Hinton, G. E., Salakhutdinov, R. R. Reducing the dimensionality of data with neural networks. *Science*, 2006, 313: 504-507.
- Hsieh, F. S., Vega, C., Vega, L. Applying a time-dependent Darcy equation for decline analysis for wells of varying reservoir type. Paper SPE 71036 Presented at SPE Rocky Mountain Petroleum Technology Conference, Keystone, Colorado, 21-23 May, 2001.
- Hughes, J. D. Energy: A reality check on the shale revolution. *Nature*, 2013, 494(7437): 307-308.
- Ji, B. Some understandings on the development trend in research of oil and gas reservoir engineering methods. *Acta Petrolei Sinica*, 2020, 41(12): 1774-1778. (in Chinese)
- Khan, M. A., Jani, S. P., Kumar, A. S., et al. Machining parameter optimization using Adam-Gene Algorithm while turning lightweight composite using ceramic cutting tools. *International Journal of Lightweight Materials and Manufacture*, 2021, 4(2): 262-267.
- Khamidullin, M., Mazo, A., Potashev, K. Numerical simulation of a one-phase steady flow towards a multistage fractured horizontal well. *Lobachevskii Journal of Mathematics*, 2017, 38(5): 818-826.
- Kuang, L., Liu, H., Ren, Y., et al. Application and development trend of artificial intelligence in petroleum exploration and development. *Petroleum Exploration and Development*, 2021, 48(1): 1-11.

- Lee, K., Lim, J., Yoon, D., et al. Prediction of shale-gas production at duvernay formation using deep-learning algorithm. *SPE Journal*, 2019, 24(6): 2423-2437.
- Li, G., Qin, J., Xian, C., et al. Theoretical understandings, key technologies and practices of tight conglomerate oilfield efficient development: A case study of the Mahu oilfield, Junggar Basin, NW China. *Petroleum Exploration and Development*, 2020, 47(6): 1185-1197.
- Liang, H., Zhang, L., Zhao, Y., et al. Empirical methods of decline-curve analysis for shale gas reservoirs: Review, evaluation, and application. *Journal of Natural Gas Science and Engineering*, 2020, 83(5): 103531.
- Liu, Y., Ma, X., Zhang, X., et al. A deep-learning-based prediction method of the estimated ultimate recovery (EUR) of shale gas wells. *Petroleum Science*, 2021, 18(5): 1450-1464.
- Luo, S., Zhao, Y., Zhang, L., et al. Integrated simulation for hydraulic fracturing, productivity prediction, and optimization in tight conglomerate reservoirs. *Energy & Fuels*, 2021, 35(18): 14658-14670.
- Mattar, L., Mcneil, R. The flowing gas material balance. *Journal of Canadian Petroleum Technology*, 1998, 37(2): 52-55.
- Meng, M., Chen, Z., Liao, X., et al. A well-testing method for parameter evaluation of multiple fractured horizontal wells with non-uniform fractures in shale oil reservoirs. *Advances in Geo-Energy Research*, 2020, 4(2): 187-198.
- Mohaghegh, S. D. Reservoir simulation and modeling based on artificial intelligence and data mining (AI&DM). *Journal of Natural Gas Science and Engineering*, 2011, 3(6): 697-705.
- Niu, W., Lu, J., Sun, Y. Development of shale gas production prediction models based on machine learning using early data. *Energy Reports*, 2022, 8: 1229-1237.
- Qin, J., Zhang, J., Jiang, Q., et al. Sweet spot classification evaluation of tight conglomerate reservoir in Mahu Sag and its engineering application. *China Petroleum Exploration*, 2020, 25(2): 110-119. (in Chinese)
- Srivastava, N., Hinton, G., Krizhevsky, A., et al. Dropout: A simple way to prevent neural networks from overfitting. *Journal of Machine Learning Research*, 2014, 15(1): 1929-1958.
- Stalgorova, E., Mattar, L. Analytical model for unconventional multifractured composite systems. *SPE Reservoir Evaluation & Engineering*, 2013, 16(3): 246-256.
- Valko, P. P. Assigning value to stimulation in the Barnett Shale: A simultaneous analysis of 7000 plus production histories and well completion records. Paper SPE 119369 Presented at SPE Hydraulic Fracturing Technology Conference, The Woodlands, Texas, USA, 19-21 January, 2009.
- Wang, K., Li, H., Wang, J., et al. Predicting production and estimated ultimate recoveries for shale gas wells: A new methodology approach. *Applied Energy*, 2017, 206: 1416-1431.
- Wang, S., Chen, Z., Chen, S. Applicability of deep neural networks on production forecasting in Bakken shale reservoirs. *Journal of Petroleum Science and Engineering*, 2019, 179: 112-125.
- Wood, D. A. Gamma-ray log derivative and volatility attributes assist facies characterization in clastic sedimentary sequences for formulaic and machine learning analysis. *Advances in Geo-Energy Research*, 2022, 6(1): 69-85.
- Yavari, H., Khosravian, R., Wood, D. A., et al. Application of mathematical and machine learning models to predict differential pressure of autonomous downhole inflow control devices. *Advances in Geo-Energy Research*, 2021, 5(4): 386-406.
- Zhou, Z. *Machine learning*. Beijing, China, Tsinghua University Press, 2016. (in Chinese)